Published in final edited form as:
Development. 2008 May ; 135(10): 1887–1895. doi:10.1242/dev.016147.

Intracardiac septation requires hedgehog-dependent cellular contributions from outside the heart

Matthew M. Goddeeris[1,*], **Silvia Rho**[1,2], **Alexandra Petiet**[3], **Chandra L. Davenport**[1], **G. Allan Johnson**[3], **Erik N. Meyers**[1,2,†], and **John Klingensmith**[1,2,‡]

[1] Department of Cell Biology,, Duke University Medical Center, Durham, NC, USA

[2] Department of Pediatrics, Duke University Medical Center, Durham, NC, USA

[3] Center for In Vivo Microscopy, Duke University Medical Center, Durham, NC, USA

Abstract

Septation of the mammalian heart into four chambers requires the orchestration of multiple tissue progenitors. Abnormalities in this process can result in potentially fatal atrioventricular septation defects (AVSD). The contribution of extracardiac cells to atrial septation has recently been recognized. Here, we use a genetic marker and novel magnetic resonance microscopy techniques to demonstrate the origins of the dorsal mesenchymal protrusion in the dorsal mesocardium, and its substantial contribution to atrioventricular septation. We explore the functional significance of this tissue to atrioventricular septation through study of the previously uncharacterized AVSD phenotype of *Shh*$^{-/-}$ mutant mouse embryos. We demonstrate that Shh signaling is required within the dorsal mesocardium for its contribution to the atria. Failure of this addition results in severe AVSD. These studies demonstrate that AVSD can result from a primary defect in dorsal mesocardium, providing a new paradigm for the understanding of human AVSD.

Keywords

Sonic hedgehog; Atrioventricular septal defect; Intracardiac septation; Heart development; Morphogenesis; Mouse

INTRODUCTION

The internal division of the heart tube into four chambers is a complex developmental process of high relevance to human congenital anomalies. Atrioventricular (AV) septation includes separation of the left and right atria from ventricles, and formation of the mitral and tricuspid valves (Lamers and Moorman, 2002). AV septation defects (AVSDs) occur in over 1 in 2800 live births, with highly variable presentation (Hoffman, 1995; Hoffman and Kaplan, 2002). The three defects most common to AVSD are atrial septum primum defect, membranous ventricular septum defect, and abnormal or missing AV valve septal leaflets. The combined effect is juncture among all four chambers of the heart, resulting in mixing of freshly oxygenated and oxygen-depleted blood.

‡Author for correspondence (kling@cellbio.duke.edu).
*Present address: Department of Molecular Physiology and Biophysics, University of Iowa, Iowa City, IA, USA
†Present address: St Luke's Children's Hospital, Boise, ID, USA

Supplementary material
Supplementary material for this article is available at http://dev.biologists.org/cgi/content/full/135/??/????/DC1

Our understanding of the process of AV septation comes in part from study of the mouse embryo. At embryonic day (E) 9.0, the interface between the atria and ventricles becomes specified as the AV canal, and formation of endocardial cushions begins. Two AV cushions form as a result of epithelial to mesenchymal transition and subsequent proliferation. The cushions themselves undergo extensive remodeling to contribute to the septal leaflets of the mitral and tricuspid valves, as well as to a large region of the membranous ventricular septum. In addition to AV cushions, the AV septal complex also includes outflow tract (OFT) endocardial cushions, the muscular ventricular septum and components of the atrial septa (reviewed by Lamers and Moorman, 2002).

The complicated process of atrial septation and its impact on AV septation is an emergent body of research. Recent work has focused on the extracardiac contribution to atrial septation by the dorsal mesocardium (DM), the region of the splanchnic mesoderm ventral to the endodermal tube and dorsal to the heart that maintains contact with the venous pole of the heart tube throughout development. Starting at E10.5, mesenchymal cells from the DM enter the atria at the site of pulmonary vein formation (Webb et al., 1998). The primary atrial septum, a myocardial extension of the dorsal atrial wall that becomes capped by mesenchyme, is already present. Webb et al. (Webb et al., 1998) re-examined via histology the contribution of DM to an atrial structure identified originally by Wilhelm His as the spina vestibuli (His, 1880), and suggested that this extracardiac tissue has a significant contribution to atrial septation. Wessels and colleagues found a similar ‘dorsal mesenchymal protrusion’ (DMP) in human embryos, composed of mesenchyme entering the heart between the pulmonary ridges at the site of future pulmonary vein formation (Wessels et al., 2000). These authors suggested that this tissue contributes to the mesenchyme capping the primary atrial septum, and helps to close the primary atrial foramen by filling the space between the primary atrial septum and AV cushions. Studies of transgenic markers of gene expression in mesenchymal cells have provided further support for a discrete contribution from the DM to the septal complex (Mommersteeg et al., 2006; Snarr et al., 2007). Here we refer to this structure descriptively as the DMP.

The identification of the DMP as a source of cells contributing to atrial septation raises many questions. For example, what is the structural contribution of the DMP to atrial septation, and more broadly to AV septation? Does the DMP functionally interact with other components of the AV complex? What genetic pathways are important for DMP development? Can defective DMP development result in AVSD? To address these questions, we use a multi-technique approach. We report a genetic marker for the DM, and use novel imaging techniques to address its morphogenesis and ultimate contribution to AV septation. We then use this knowledge to address the functional relevance of the DMP to the pathogenesis of an uncharacterized mouse model of AVSD, demonstrating a crucial role for hedgehog signaling in this process.

MATERIALS AND METHODS

Mouse lines and generation of conditional mutants

Mice were maintained on an outbred ICR genetic background. *Shh*$^{er\text{-}Cre}$ produces a fusion protein of Cre with human estrogen receptor targeted to the *Shh* locus (*Shh*$^{tm2(cre/ESR1)Cjt}$) (Harfe et al., 2004). Descriptions of remaining mouse lines used here can be found in Goddeeris et al. (Goddeeris et al., 2007). Noon of the day of vaginal plug detection was defined as embryonic day (E) 0.5. Embryos were genotyped for *Cre* (Meyers et al., 1998) and for the *Smo* wild-type and flox alleles (Zhang et al., 2001). In all figures, wild-type (WT) refers to littermates that are either Cre(+) and flox/+, or flox/flox but Cre (−), unless otherwise specified.

Immunohistochemistry and β-galactosidase detection

Histological preparation of embryos followed standard procedures (Goddeeris et al., 2007; Hogan et al., 1994). Section immunohistochemistry was conducted on sagittal paraffin sections (8 μM) incubated with rat anti-PECAM-1 (1:250; PharMingen, CN557355) or rabbit anti-phosphorylated histone H3 antibody (1:250; Upstate Biotechnology). Anti-phosphorylated histone H3 signal was amplified with biotinylated anti-rabbit (Vector Labs). Detection was with Cy3 conjugated streptavidin (Vector Labs, 1:250) and Cy5 conjugated anti-rat (Jackson Immuno, 1:250). Nucleus detection was with Syto13 (Invitrogen, 1:1000) in PBT. Undiluted MF-20 supernatant (Developmental Studies Hybridoma Bank) was used with methanol-fixed embryos and detected with rhodamine red-conjugated goat anti-mouse IgG, Fcγ subclass 2b specific secondary (Jackson Immunoresearch) followed by paraffin sectioning and nuclei detection with Syto13. Lysotracker Red cell death analysis was as described (Abu-Issa et al., 2002; Zucker et al., 1999). Whole-mount in situ hybridization with digoxigenin-labeled riboprobes was as described (Neubuser et al., 1997). The *Shh* riboprobe has been previously reported (Echelard et al., 1993).

Confocal microscopy was performed on a Zeiss LSM 510 META. Images were prepared in Adobe Photoshop 7.0.1. Control and mutant images were treated identically and represent the data set as a whole. Manual mesenchyme cell counts were analyzed by Student's *t*-test. Volume was measured using ImageJ Freeware (1.37v, NIH).

Transwell explant cultures

Dorsal mesocardium was dissected from E10.5 ICR embryos and cultured on rat type 1 collagen for 24 hours at 37°C in DMEM with 10% fetal calf serum (FCS). Pooled explants were dissociated with trypsin, washed and resuspended in 500 μL OPTI-MEM/1% FCS. 15,000 cells in 100 μL OPTI-MEM/1% FCS were added to each transwell insert (Costar 3422) coated with type 1 collagen and placed in a 24-well plate. Each bottom well was filled with 600 μL DMEM/10% FCS. In some wells, 10 μM cyclopamine in DMSO was added. Control cells were treated with DMSO, or cultured in media alone. Cells were incubated at 37°C for 48 hours. Cells on the underside of the transwell insert membrane were fixed and stained with Gills #1 Hematoxylin and Eosin.

MRM

Embryos were imaged at E14. Contrast procedures and imaging were as described (Petiet et al., 2007), using a vertical bore 9.4T magnet interfaced to a GE EXCITE console, modified for MRM through an intermediate stage in the radiofrequency (rf) chain. Images were acquired using 3D rf refocused spin warp encoding with extended dynamic range (Johnson et al., 2007) yielding 3D image arrays of 512×512×1024 with isotropic spatial resolution of 19.5 μm^3. Acquisition time was 4 hours. Hearts were color-labeled and segmented using VoxPort Software by MRPath (Durham, NC) and a Matlab routine. Volume-rendered images were generated using VGStudio Max by Volume Graphics GmbH (Germany).

RESULTS

We have previously demonstrated that sonic hedgehog (Shh) signaling is essential for the contribution of the anterior heart field (AHF) to the developing OFT (Goddeeris et al., 2007). The AHF includes a splanchnic mesodermal region that contributes to the arterial pole of the primary heart tube to form much of the OFT and right ventricle (Kelly et al., 2001; Mjaatvedt et al., 2001; Waldo et al., 2001). Intriguingly, expression of AHF markers also has been described in or near the developing atria, supporting the view that this domain contributes to both the arterial and venous poles of the primary heart tube (Cai et al., 2003; Huynh et al., 2007; Kelly et al., 2001; Mommersteeg et al., 2006; Snarr et al., 2007). In the course of our

previous studies, we noted similar atrial expression with the *Cre* transgenic line *Mef2C-AHF-Cre* (Verzi et al., 2005) using the Cre recombination reporter *R26R* (Soriano, 1999), which indicates where recombination has occurred via β-galactosidase (β-gal) expression. The atrial expression pattern includes regions of the atrial septum thought to be of extracardiac mesenchymal origin, specifically the DMP. As little is understood about the nature of this tissue, we sought to address its origin and contributions to atrial septation using *Mef2C-AHF-Cre* as a genetic tool.

We crossed *Mef2C-AHF-Cre* with *R26R* in a series of pseudo-lineage trace experiments to determine the extent to which this cell population contributes to AV septation in later stages of heart development. By E10.5, this *Cre* line leads to β-gal expression in the splanchnic mesoderm, which is continuous with the DM (Fig. 1A, B). *Mef2C-AHF-Cre* was also observed in the medial dorsal myocardial wall of the atria continuous with the splanchnic mesoderm. By E11.5, *R26R* expressing mesenchymal cells continuous with the DM are seen to protrude into the atria at the future point of pulmonary vein attachment. This DMP expression domain extends to the inferior AV cushion, and comprises part of the mesenchymal cap that extends to the superior AV cushion (Fig. 1C). This pattern indicates that *Mef2C-AHF-Cre* is either expressed in the DMP and mesenchymal cap, or that these tissues are derived from tissue that once expressed *Cre*, such as the DM.

In embryos from E12.5–E16.5, cells derived from the *Mef2C-AHF-Cre* expression domain constitute much of the tissue continuous with the AV cushion-derived central mesenchymal mass, as well as much of the primary atrial septum (Fig. 1D–F). Cre expression is specific to this midline tissue and largely excludes AV cushion-derived mesenchyme. At E14.5, labeled cells were observed continuous with the primary atrial septum, forming a wedge over the fused AV cushion-derived tissue. By this stage, the AV cushion tissue has redistributed to form the septal leaflets of the mitral and tricuspid valves. In summary, histological analysis suggests that the primary atrial septum is partially derived from *Mef2C-AHF-Cre*-positive cells.

Using magnetic resonance microscopy (MRM) of E14.5 embryos in comparison to *Mef2C-AHF-Cre; R26R* embryos, we generated three-dimensional (3D) renderings of the *Mef2C-AHF-Cre* lineage contribution to the atrial septum. Heart structures were color-labeled from the MRM slices according to the pattern observed in closely matched *Mef2C-AHF-Cre; R26R* sections (Fig. 1G). These heart structures were isolated and recompiled to generate a 3D structure (Petiet et al., 2007). Multiple views suggest that these labeled cells contribute much of the atrial septal complex and present a large interface with the remodeling AV cushions (Fig. 1H). Near the dorsal atrial wall, cells derived from the *Mef2C-AHF-Cre* domain occupy a greater volume than the remaining component of the primary atrial septum. Together, these data confirm that the DMP is derived from the DM, and show that the DMP in turn gives rise to much of the tissue mass in the atrial septal complex.

Hh responsive DMP is deficient in *Shh*$^{-/-}$ mutant embryos

As the pathogenic mechanisms of many AVSDs are unclear, we wished to determine whether abnormal DMP development could be a causal defect. Besides OFT phenotypes, *Shh*$^{-/-}$ mutant embryos have ventricular and atrial septal defects (Washington Smoak et al., 2005), as well as incompletely-penetrant AVSD with a single AV valve (Fig. 2A, B). Most *Shh*$^{-/-}$ mutants have rudimentary septal AV valve leaflets, though some lack even these. The causes of the large atrial septation defect observed in *Shh*$^{-/-}$ mutants have not been addressed, but the phenotype is consistent with the absence of tissue from the AV septal complex. Recent data indicate that the ventral pharyngeal endoderm (PE) is the source of Shh required for normal OFT development (Goddeeris et al., 2007), but there are no overt domains of *Shh* expression within the heart to explain a role in AV septation. We therefore investigated this apparent contradiction.

First, we further assessed the potential Shh source relevant for AV septation. There are no detectable areas of *Shh* expression within the OFT, ventricles or atria, as assayed by whole-mount in situ hybridization, RT-PCR or $Shh^{er\text{-}Cre}$*; R26R* analysis from E9.5 to E11.5 (Fig. 2C) (Goddeeris et al., 2007). However, the ventral PE expresses *Shh* and is juxtaposed to the dorsal mesocardium during DMP formation (Fig. 2D). Consistent with this observation, we have previously demonstrated that loss of *Shh* from the PE results in AVSD (Goddeeris et al., 2007). The lack of overt *Shh* expression within the heart itself and the presence of AVSD in embryos lacking endodermal *Shh* led us to hypothesize that Shh produced in the PE acts on the DM, which in turn forms the DMP and contributes to atrial septation.

Shh is one of three mammalian hedgehog (Hh) ligands, the signal transduction of which is positively effected in responsive cells by a receptor, smoothened (Smo). It is negatively regulated by patched 1 (Ptch1), a positive transcriptional target widely used to report Hh signaling activity (Ingham and McMahon, 2001). $Ptch1^{lacZ}$ activity appears to be restricted to the developing atria and distal OFT myocardium (Fig. 2E, F) (Washington Smoak et al., 2005). Atrial expression is first observed at E10.5 in the DM near the pulmonary pit (data not shown). At later stages (E11.5–E13.5), weak expression is observed in the DMP within the atria (Fig. 2E, F). This *Ptch1* domain is *Shh* dependent, as $Shh^{-/-}$ embryos lack $Ptch1^{lacZ}$ expression within the atria (Fig. 2G, H; see Fig. S1 in the supplementary material). Thus, the DMP is the only component of the AV septation complex with detectable, *Shh*-dependent, $Ptch1^{lacZ}$ expression.

Early development of the AV cushions does not require Shh signaling

Classical models for the etiology of AVSD have focused on early abnormalities in AV cushion development. To see whether these pertain to $Shh^{-/-}$ mutants, we conducted histological analysis at early stages in AV formation (E9.5–E11.5), a hallmark of which is epithelial to mesenchymal transition (EMT) of endocardial cells to populate the cardiac jelly.

The AV cushions appeared normal in size and morphology at E9.5. Appropriate numbers of mesenchymal cells were present in the cushion cardiac jelly (data not shown), suggesting that AV cushion specification and the initial events of EMT proceed normally in the AV canal of $Shh^{-/-}$ embryos. To assess the subsequent extent of EMT, we performed section immunohistochemistry on $Shh^{-/-}$ mutants and wild-type littermates at E10.5 and E11.5 (Fig. 3A, B). Cushion mesenchymal cells were assessed by location and lack of the endothelial marker Pecam1, and counted in serial sections through a given embryo. No significant difference in total cell number was found in either cushion at E10.5 (Fig. 3C) or E11.5 (data not shown). Cell proliferation was assayed by immunodetection of phosphorylated histone H3. No difference was observed in E10.5 AV cushion proliferation (data not shown) or total AV cushion volume (Fig. 3D) between wild type and $Shh^{-/-}$ mutants. Together, these data indicate early stages of AV cushion formation and growth are normal despite loss of *Shh*.

By E14.5, AV cushion structure is abnormal in Shh mutants (Fig. 2B); thus, it is possible that disrupted Hh signaling during later stages of AV cushion development might play an important role in generating AVSD. On the other hand, our phenotypic analysis, combined with the observation that the DM and DMP are Shh responsive, suggests that loss of the DMP may be part of the etiology of $Shh^{-/-}$ AVSD. Such considerations suggested three hypotheses: (1) that defective Hh signaling in the AV cushions causes defects not only in this tissue but in AV septation in general; (2) loss of Hh signaling in the developing DMP alone is sufficient to recapitulate the full AVSD; or (3) defective signaling in both DMP and AV cushion development lead to the $Shh^{-/-}$ AVSD phenotype. To distinguish between these possibilities, we used tissue-specific gene ablation to disrupt Hh signaling.

Neither endocardium nor myocardium requires direct Hh signaling for AV septation

To test whether direct Hh signaling to the developing AV cushions is required for normal AV septation, we ablated the *Smo* receptor, and thus Hh receptiveness, from the two primary tissues of the AV cushions: the myocardium, the endocardium, or both, in combination, then analyzed mutant embryos for AVSD. To test necessity of Hh signaling in the myocardium, we generated mutants of the genotype *TnT-Cre; Smo*$^{flox/-}$. *TnT-Cre* is expressed throughout the differentiated myocardium of the heart but not in the endocardium (Jiao et al., 2003) (Fig. 4A, A′). All mutants sectioned (7/7) had normal AV septation (Fig. 4B). Thus, loss of Hh signaling to the myocardium fails to recapitulate the *Shh*$^{-/-}$ AVSD phenotype. Interestingly, *R26R* analysis of *TnT-Cre* expression at E11.5 and later stages revealed *TnT-Cre* expression at the leading edge of the DMP (data not shown), consistent with observations that this mesenchyme becomes myocardial after entry into the atria (Soufan et al., 2004). As *TnT-Cre; Smo*$^{flox/-}$ mutants have no atrial septation defects, we conclude that Hh signaling to the DMP is not required after differentiation into myocardium.

We next tested whether the endocardium requires a direct Hh signal. We ablated *Smo* from the endocardium using *Tie2-Cre* (Fig. 4C, C′) (Koni et al., 2001). As the AV cushion mesenchyme is derived from the endocardium, this tissue also lacks *Smo*. Histological analysis at late stages revealed no intracardiac defects in these mutants (9/9, Fig. 4D), indicating that the endocardium and its derivatives do not require Hh signaling for normal AV septation.

Given these results, we could not rule out the possibility that loss of signaling to both tissues was necessary to induce the defect. We therefore generated a double *Cre* transgenic line using both *TnT-Cre* and *Tie2-Cre*. These embryos have the combined expression pattern of *TnT-Cre* and *Tie2-Cre* as detected by *R26R* (Fig. 4E, E′). By section analysis, we found normal AV septation in *TnT-Cre; Tie2-Cre; Smo*$^{flox/-}$ mutant embryos (6/6, Fig. 4F). When combined, these results indicate that neither AV cushion myocardium, endocardium nor the combination of the two require direct Hh signaling for normal AV septation. Notably, the DM does not demonstrate *Cre* expression in any of these mutant classes, further suggesting that the AV canal defects in *Shh*$^{-/-}$ embryos are not related to the direct loss of Hh signaling to the AV cushions.

Mef2C-AHF-Cre; Smo$^{flox/-}$ mutants recapitulate *Shh*$^{-/-}$ intracardiac septation defects

To test whether Hh signaling is required within the DM for heart septation, we generated *Mef2C-AHF-Cre; Smo*$^{flox/-}$ embryos. This strategy removed the ability of the DM to respond to Shh from the pharyngeal endoderm. These embryos survive to term with a failure in OFT septation (Goddeeris et al., 2007). In addition to this phenotype, section analysis of mutant and wild-type embryos between E14.5 and E18.5 revealed intracardiac defects consistent with those found in *Shh*$^{-/-}$ mutants (Fig. 5A, B). All *Mef2C-AHF-Cre; Smo*$^{flox/-}$ mutants observed (15/15) had a large atrial septation defect as well as a pronounced VSD at the level of the OFT-ventricle connection. The atrial septation defect is consistent with loss of the DMP (Fig. 5A–D). Typically, the muscular primary atrial septum was observed along the dorsal-most atrial wall (data not shown). In addition to atrial septation defects, most *Mef2C-AHF-Cre; Smo*$^{flox/-}$ mutants (11/15) have abnormally short, rounded septal AV valve leaflets. In most cases, the central mass of mesenchyme affixed to the muscular ventricular septum appeared much larger and more rounded than in control embryos (Fig. 5B, D). This mass is probably comprised entirely of AV cushion-derived tissue, as it is not β-gal positive in *Mef2C-AHF-Cre; Smo*$^{flox/-}$*; R26R* embryos (Fig. 5B). The most severe forms of AVSD found at low penetrance in *Shh*$^{-/-}$ mutants, i.e. lack of all septal leaflets of the AV valves and the central mesenchymal mass, were not observed in *Mef2C-AHF-Cre, Smo*$^{flox/-}$ mutants. These results indicate that the DM requires Hh signaling for intracardiac septation and that loss of receptiveness within this domain can largely recapitulate the AV septation defects observed in *Shh*$^{-/-}$ embryos.

To better characterize the *Mef2C-AHF-Cre; Smo$^{flox/-}$* mutant class, we used MRM imaging in comparison with stage-matched, E14.5 lineage traced embryo sections to generate color-labeled heart renderings. These structures confirmed the absence of the DMP and subsequent large atrial septation defect in these mutants (Fig. 5E–F′). Complete sets of MRM serial slices of *Mef2C-AHF-Cre; Smo$^{flox/-}$*, *Shh$^{-/-}$*, and wild-type controls are available for reference online (http://www.civm.duhs.duke.edu/dev01/index.html).

Taken together, our tissue-specific ablations indicate that the DMP is essential for intracardiac septation. Hh signaling is necessary within the DM for DMP morphogenesis and contribution to the septal complex. Moreover, absence of the DMP contribution has an indirect effect on the morphology of AV cushions.

Loss of Hh signaling results in abnormal DM differentiation and migration

To understand the early etiology of the AVSD in *Mef2C-AHF-Cre; Smo$^{flox/-}$* embryos, we characterized the distribution of β-gal positive cells in *Mef2C-AHF-Cre; Smo$^{flox/-}$;R26R* and control embryos. At E10.5, no differences in the total amount or location of β-gal positive cells were observed (Fig. 6A, B). However, far fewer mesenchymal cells were observed within the atria of mutant embryos at E11.5 relative to wild-type littermates (Fig. 6C, D). At E10.5 and E11.5 there appeared to be an increase in midline β-gal positive atrial myocardial cells. However, increased *Mef2C-AHF-Cre* contribution to the atrial myocardium was not detectable at E14.5 and later stages (Fig. 5A, B and data not shown). These data indicate that although an adequate population of DM cells is present at E10.5 in mutants, it is not capable of DMP formation.

Next we analyzed whether loss of Hh signaling in the DM affects proliferation, cell death, differentiation or migration. Analysis of proliferation in *Mef2C-AHF-Cre; Smo$^{flox/-}$* embryos was assessed via anti-phosphorylated histone H3 antibody detection; no differences were observed in the DM (data not shown). Cell death was assayed using the Lysotracker Red fluorescent probe, a lysosomal marker, at E10.5 and E11.5. No differences in cell death within the DM or atria were observed comparing *Mef2C-AHF-Cre; Smo$^{flox/-}$* embryos with control littermates (Fig. 6E–H). Together, these data suggest that loss of DMP tissue in *Mef2C-AHF-Cre; Smo$^{flox/-}$* embryos is not the result of decreased proliferation or increased cell death within the DM at these stages.

As discussed here and previously (Soufan et al., 2004), a region of the DMP undergoes differentiation into myocardium after its formation. One possible explanation for abnormal DMP development is abnormal control of differentiation. We addressed this possibility by testing for the presence of striated muscle specific myosin using the myofilament-20 (MF-20) antibody in E11.5 embryos (Bader et al., 1982). We observed the presence of MF-20 positive cells within the splanchnic mesoderm and DM of *Mef2C-AHF-Cre; Smo$^{flox/-}$* mutants (Fig. 6I–J′). MF-20 positive cells were never observed outside of the heart in the body wall in wild-type controls (Fig. 6I′). Therefore, inappropriate differentiation may contribute to the loss of DMP formation in these mutants.

Another mechanism for the DMP defect might be a reduction in the ability of DM cells to move into the atria, for example by compromised migration. To address this possibility, we employed a transwell migration assay (see Materials and methods). Explanted DM (and closely adherent tissues) from E10.5 wild-type embryos was assayed for migratory properties. Three migration culture conditions were tested using the same starting population of DM cells: media only, 10 μM cyclopamine [a small molecule Smo inhibitor (Chen et al., 2002)] and a DMSO (cyclopamine carrier) control. We observed a 37% reduction in migration with cyclopamine treatment compared with the DMSO control treatment (P=0.001, n=3, Fig. 6K). Therefore, in

addition to inappropriate differentiation of DM cells, another cellular cause of the defect may be a reduction in their migratory capability.

Abnormal AV cushion rightward expansion and DMP development in *Shh*$^{-/-}$ mutants

Relative to *Mef2C-AHF-Cre; Smo*$^{flox/-}$ embryos, *Shh*$^{-/-}$ mutants tend to have more severe cases of AVSD, exemplified by the complete lack of septal AV valves and a central mesenchymal mass. Accordingly, we analyzed *Shh*$^{-/-}$ mutants for additional AV complex defects. Although differences in cell number were not found, abnormalities in AV cushion shape were detectable by section analysis in *Shh*$^{-/-}$ mutants. At E11.5, a pronounced shape change was observed in both the superior and inferior cushions in some embryos. The inferior cushion appears less rounded than in wild-type embryos while the superior cushion is elongated or stretched. We were able to demonstrate this shift graphically by plotting the cushion surface area of consecutive sagittal sections (see Fig. S2 in the supplementary material). This shape change reduces the amount of superior AV cushion tissue present at the midline of the heart, where the cushions interact with the DMP and primary atrial septum, implying a role for Hh in AV cushion rightward expansion. However, this role must be indirect, as this phenotype was not observed in the simultaneous conditional ablations of *Smo* in the myocardium and endocardium. We suggest that this abnormal AV cushion distribution in *Shh*$^{-/-}$ mutants is the result of OFT and right ventricle shortening (Washington Smoak et al., 2005), causing general disrupted heart curvature. Consistent with this, *Mef2C-AHF-Cre; Smo*$^{flox/-}$ embryos (which have relatively normal OFT and right ventricle length) were not observed to have abnormal AV cushion shape or distribution (data not shown), suggesting normal OFT lengthening is required for proper AV cushion rightward expansion. Together, these data imply that a combination of defective AV cushion rightward expansion and DMP development culminates in the most severe forms of AVSD in *Shh*$^{-/-}$ mutants.

DISCUSSION

Conventional understanding of the etiology of AVSDs has largely focused on abnormal development of the AV cushions. However, new findings suggest that AVSDs seen in perinatal humans are more complex in their origins. Previous work has demonstrated that deficient DMP development occurs in mouse (Webb et al., 1999) and human (Blom et al., 2003) fetuses with AVSD. As such individuals exhibit malformations in other septal structures, the specific role of DMP defects in generating these malformations has been unclear. Here, we show that the DMP is crucial for atrial and AV valve development. We demonstrate that AVSD can arise from a primary defect in the DMP, rather than in the AV cushions. These studies support a new paradigm for understanding the pathogenic mechanisms of AVSD.

Mef2C-AHF-Cre activity marks extracardiac contributions to the primary atrial septum

Recently, several groups have recognized the late extra-cardiac contribution of the DM to the atria (Mommersteeg et al., 2006; Webb et al., 1998; Wessels et al., 2000). These studies found that continuous with the DM, the DMP expands into the atria and wedges to close the gap formed between the primary atrial septum and the AV cushion mesenchyme. However, owing to a lack of adequate markers for this population, direct confirmation of these observations and assessment of DMP contribution to later atrial development has been difficult. We demonstrate that *Mef2C-AHF-Cre* is a faithful marker for the DM and its contribution to atrial septation.

From our pseudo-lineage trace and MRM analysis, we confirm that DM enters the developing atria at the site of pulmonary vein formation. The resulting mesenchymal mass, the DMP, elongates to fuse with the inferior AV cushion. *Mef2C-AHF-Cre* cells make up a region of the ‘mesenchymal cap’ of the primary atrial septum, which directly fuses with the superior AV cushion (Fig. 7A). These findings are consistent with previous models (Lamers and Moorman,

2002;Wessels et al., 2000). Loss of Hh signaling affects both the DMP and mesenchymal cap of the primary atrial septum, consistent with a common origin of these tissues.

The specificity of *Mef2C-AHF-Cre* allowed for the analysis of DMP contributions to later stages of atrial development. As visualized by MRM, the DMP maintains a large and clearly demarcated interface with the tissue derived from the AV cushions. We observed *Mef2C-AHF-Cre; R26R* expressing cells in the dorsal-medial myocardium of the atria. We suggest that splanchnic mesodermal derivatives distinct from the DMP add to the atria during the same time frame as the DMP. However, in contrast to the DMP, these cells do not directly require Hh signaling, as they are still present in *Mef2C-AHF-Cre; Smo*$^{flox/-}$ mutants. Alternatively, these cells may independently express the *Mef2C-AHF-Cre* transgene at this point in development.

The DMP is an outgrowth into the atrial lumen from the DM, in turn composed largely of mesenchyme ventral to the foregut. Given that *Mef2C-AHF-Cre* activity results in recombined cells in both the DMP and splanchnic mesoderm, it is conceivable that these tissues arise from a common precursor. We note that DMP labeling by cells from the *Mef2C-AHF-Cre* expression domain is probably not unique to this particular AHF-Cre driver, as similar atrial expression has been reported in studies of other mouse genes expressed in the AHF, such as *Fgf10*, *Isl1* and *Tbx1* (Cai et al., 2003; Huynh et al., 2007; Kelly et al., 2001; Mommersteeg et al., 2006; Snarr et al., 2007).

AVSD can result directly from DMP defects

To address whether the DMP is necessary for atrial septation and to further explore its role in AV septation, we identified a mouse mutant in which this structure is defective. *Shh*$^{-/-}$ mutants suffer from a severe atrial septal defect and AVSD, and Hh responsiveness occurs endogenously in the DM (Fig. 7B). Results reported here and previously (Goddeeris et al., 2007) imply that Shh signaling from the foregut endoderm is required for normal AV septation, as it is the only relevant domain of *Shh* expression. This relatively distant ligand source elicits its effect on AV septation by being juxtaposed to the DM prior to its contribution to the AV complex. We demonstrate that *Ptch1*^{lacZ} is expressed within the DM and that Cre-mediated loss of Hh receptiveness within the *Mef2C-AHF-Cre* expression domain is sufficient to recapitulate the consequences of absent Shh ligand on septal development (Fig. 7D).

Little is understood concerning the mechanism by which the DM enters the atria, and several possibilities might underlie the mechanism underlying the DMP defect. First, Shh produced by foregut endoderm may signal directly to the DM to elevate levels of proliferation, thus providing a sufficient population of cells to form the DMP. Although we were unable to observe proliferation differences in *Mef2C-AHF-Cre; Smo*$^{flox/-}$ mutant DM, such differences may occur at time points not studied here. Alternatively, Shh may promote cell shape changes or the coordinated migration of DM cells into the atria, resulting in an actual ‘protrusion’ into the lumen. Equally plausible is that a combination of both migration and proliferation is responsible. In tissue culture assays, we found a reduction of over 35% in migrating DM cells after 24 hours of Hh inhibition. Perhaps a prolonged reduction of Hh signaling (as in the mutants in vivo) would increase the level of migration inhibition, accounting for the severe DMP deficiency. Finally, we detected DM cells that express the myofibril marker MF-20 within the body wall of E11.5 *Mef2C-AHF-Cre; Smo*$^{flox/-}$ mutants. Normally, these cells should only express such markers after they have entered the atria. Based on this surprising result, we suggest two possible explanations. DM cells may require Hh signaling to repress actively the expression of myocardial differentiation genes, and loss of this signaling results in premature differentiation of cells en route to the atrial compartment. Alternatively, the DM we observed in mutants may be differentiating in the normal time frame, but in an inappropriate location owing to a cell-motility defect.

A surprising finding is the role of the DMP in AV cushion maturation. The AV valves are completely derived from tissues unrelated to the DMP and theoretically should not be affected (de Lange et al., 2004). Nevertheless, discrete loss of the DMP results in severe defects in AV valve formation. *Shh*$^{-/-}$ and *Mef2C-AHF-Cre; Smo*$^{flox/-}$ mutant embryos each had abnormal AV valve development, for which several possibilities exist. The DMP may provide remodeling signals to the AV cushion mesenchyme that are crucial to AV valve formation. Alternatively, the DMP may provide a physical force, pressing the AV mesenchyme into its proper conformation. We observed the central AV mesenchymal mass to be abnormally large and rounded atop the muscular septum in multiple *Mef2C-AHF-Cre; Smo*$^{flox/-}$ mutants, consistent with both models. If loss of the DMP results in loss of a secondary signal from the DMP to the AV cushions, this secondary signal is unlikely to be a Hh ligand, as we were unable to detect any *Ptch*^{lacZ} activity within the AV cushions. Furthermore, myocardial and endocardial loss of *Smo* does not affect AV septation (Fig. 7C).

OFT defects can increase the severity of AVSDs

Mef2C-AHF-Cre; Smo$^{flox/-}$ mutant AVSDs are often less severe than those of *Shh*$^{-/-}$ embryos. This may be due to the AV cushion expansion defect we observed in some *Shh*$^{-/-}$ embryos at E11.5. In these embryos the AV cushions do not expand correctly or evenly to the right. As schematized in Fig. 7, the major cardiac phenotypic difference between these two classes of embryos is that *Shh*$^{-/-}$ embryos have a much shorter OFT and smaller right ventricle (Goddeeris et al., 2007;Washington Smoak et al., 2005). Webb et al. (Webb et al., 1999) linked a similar AV cushion expansion defect in Ts16 trisomic mouse mutants with abnormalities in the curvature of the heart tube. *Shh*$^{-/-}$ mutants have significant shortening of the right ventricle and OFT, which subsequently results in decreased outer curvature. Thus, we propose that more severe aspects of AVSD in *Shh*$^{-/-}$ embryos are the combined result of DMP developmental failure and abnormal AV cushion rightward expansion, in turn related to severe OFT and right ventricle shortening. Consistent with this connection, another class of mutants with severe AVSD, *Nkx2.5*^{Cre}*; Shh*$^{flox/-}$, has both abnormal AV cushion shape and OFT shortening (data not shown) (Goddeeris et al., 2007). *Mef2C-AHF-Cre; Smo*$^{flox/-}$ mutants, which possess relatively normal OFT and right ventricle lengthening, do not have these more severe defects.

Mef2C-AHF-Cre; Smo$^{flox/-}$ mutant intracardiac defects resemble human AVSD

Mouse models that directly impact AV cushion development typically result in embryonic lethality, limiting their clinical relevance to human AVSD. In our study of *Mef2C-AHF-Cre; Smo*$^{flox/-}$ and *Shh*$^{-/-}$ mutant AV septation defects, we found that the range of severity and constellation of AVSDs observed are consistent with those found in humans. For example, individuals with Down syndrome (Trisomy 21) have remarkably similar types of AVSD that are associated with defects in DMP expansion (Blom et al., 2003). AVSD is also observed in the Ts16 Down syndrome mouse model, in which the DMP is deficient (Webb et al., 1999; Snarr et al., 2007). Here, we demonstrate that AVSD can be the direct result of defective DMP development in mice. A broader analysis of defective DMP development in humans with AVSD is necessary to better understand the basis of these serious birth defects.

Supplementary Material

Refer to Web version on PubMed Central for supplementary material.

Acknowledgments

The authors thank B. Black and K. Jiao for providing *Mef2C-AHF-Cre* and *TnT-Cre*, respectively; R. Ilagan and M. Kirby for comments on the manuscript; B. Patton and K. Wettermark for technical assistance; and M. Lin for assistance with MRM renderings. This work was supported by NIH grants HD480305 and HL086853 to J.K. and E.N.M.; by a predoctoral AHA Grant 061543OU to M.M.G.; and by NIH/NCRR grant P41 RR005959 and NCI grant R24

CA092656 to A.E.P. and G.A.J. MF-20 was developed by D. A. Fischman and obtained from the Developmental Studies Hybridoma Bank developed under the auspices of NICHD and maintained by the University of Iowa, Department of Biological Sciences, Iowa City, IA 52242, USA.

References

Abu-Issa R, Smyth G, Smoak I, Yamamura K, Meyers EN. Fgf8 is required for pharyngeal arch and cardiovascular development in the mouse. Development 2002;129:4613–4625. [PubMed: 12223417]

Bader D, Masaki T, Fischman DA. Immunochemical analysis of myosin heavy chain during avian myogenesis in vivo and in vitro. J Cell Biol 1982;95:763–770. [PubMed: 6185504]

Blom NA, Ottenkamp J, Wenink AG, Gittenberger-de Groot AC. Deficiency of the vestibular spine in atrioventricular septal defects in human fetuses with down syndrome. Am J Cardiol 2003;91:180–184. [PubMed: 12521631]

Cai CL, Liang X, Shi Y, Chu PH, Pfaff SL, Chen J, Evans S. Isl1 identifies a cardiac progenitor population that proliferates prior to differentiation and contributes a majority of cells to the heart. Dev Cell 2003;5:877–889. [PubMed: 14667410]

Chen JK, Taipale J, Young KE, Maiti T, Beachy PA. Small molecule modulation of Smoothened activity. Proc Natl Acad Sci USA 2002;99:14071–14076. [PubMed: 12391318]

de Lange FJ, Moorman AF, Anderson RH, Manner J, Soufan AT, de Gier-de Vries C, Schneider MD, Webb S, van den Hoff MJ, Christoffels VM. Lineage and morphogenetic analysis of the cardiac valves. Circ Res 2004;95:645–654. [PubMed: 15297379]

Echelard Y, Epstein DJ, St-Jacques B, Shen L, Mohler J, McMahon JA, McMahon AP. Sonic hedgehog, a member of a family of putative signaling molecules, is implicated in the regulation of CNS polarity. Cell 1993;75:1417–1430. [PubMed: 7916661]

Goddeeris MM, Schwartz R, Klingensmith J, Meyers EN. Independent requirements for Hedgehog signaling by both the anterior heart field and neural crest cells for outflow tract development. Development 2007;134:1593–1604. [PubMed: 17344228]

Harfe BD, Scherz PJ, Nissim S, Tian H, McMahon AP, Tabin CJ. Evidence for an expansion-based temporal Shh gradient in specifying vertebrate digit identities. Cell 2004;118:517–528. [PubMed: 15315763]

His W. Die area interposita, die Eustachische klappe und die spina vestibuli. Anatomie Menschlicher Embryonen 1880;1880:149–152.

Hoffman JI. Incidence of congenital heart disease. II Prenatal incidence. Pediatr Cardiol 1995;16:155–165. [PubMed: 7567659]

Hoffman JI, Kaplan S. The incidence of congenital heart disease. J Am Coll Cardiol 2002;39:1890–1900. [PubMed: 12084585]

Hogan, B.; Beddington, R.; Constantini, F.; Lacy, E. Manipulating the Mouse Embryo: A Laboratory Manual. Plainview, NY: Cold Spring Harbor Laboratory Press; 1994.

Huynh T, Chen L, Terrell P, Baldini A. A fate map of Tbx1 expressing cells reveals heterogeneity in the second cardiac field. Genesis 2007;45:470–475. [PubMed: 17610275]

Ingham PW, McMahon AP. Hedgehog signaling in animal development: paradigms and principles. Genes Dev 2001;15:3059–3087. [PubMed: 11731473]

Jiao xxxxxxxxxxxxxxxxxxxxxxxxxxxxxxxxxxxxxxxxxxxxxxxxxxxxxxxxxxxxxxxxxxxxxxxxxxxxxxxxxx

Johnson GA, Ali-Sharief A, Badea A, Brandenburg J, Cofer G, Fubara B, Gewalt S, Hedlund LW, Upchurch L. High-throughput morphologic phenotyping of the mouse brain with magnetic resonance histology. Neuroimage 2007;37:82–89. [PubMed: 17574443]

Kelly RG, Brown NA, Buckingham ME. The arterial pole of the mouse heart forms from Fgf10-expressing cells in pharyngeal mesoderm. Dev Cell 2001;1:435–440. [PubMed: 11702954]

Koni PA, Joshi SK, Temann UA, Olson D, Burkly L, Flavell RA. Conditional vascular cell adhesion molecule 1 deletion in mice: impaired lymphocyte migration to bone marrow. J Exp Med 2001;193:741–754. [PubMed: 11257140]

Lamers WH, Moorman AF. Cardiac septation: a late contribution of the embryonic primary myocardium to heart morphogenesis. Circ Res 2002;91:93–103. [PubMed: 12142341]

Meyers EN, Lewandoski M, Martin GR. An Fgf8 mutant allelic series generated by Cre- and Flp-mediated recombination. Nat Genet 1998;18:136–141. [PubMed: 9462741]

Mjaatvedt CH, Nakaoka T, Moreno-Rodriguez R, Norris RA, Kern MJ, Eisenberg CA, Turner D, Markwald RR. The outflow tract of the heart is recruited from a novel heart-forming field. Dev Biol 2001;238:97–109. [PubMed: 11783996]

Mommersteeg MT, Soufan AT, de Lange FJ, van den Hoff MJ, Anderson RH, Christoffels VM, Moorman AF. Two distinct pools of mesenchyme contribute to the development of the atrial septum. Circ Res 2006;99:351–353. [PubMed: 16873717]

Neubuser A, Peters H, Balling R, Martin GR. Antagonistic interactions between FGF and BMP signaling pathways: a mechanism for positioning the sites of tooth formation. Cell 1997;90:247–255. [PubMed: 9244299]

Petiet A, Hedlund L, Johnson GA. Staining methods for magnetic resonance microscopy of the rat fetus. J Magn Reson Imaging 2007;25:1192–1198. [PubMed: 17520739]

Snarr BS, O'Neal JL, Chintalapudi MR, Wirrig EE, Phelps AL, Kubalak SW, Wessels A. Isl1 expression at the venous pole identifies a novel role for the second heart field in cardiac development. Circ Res 2007;101:971–974. [PubMed: 17947796]

Soriano P. Generalized lacZ expression with the ROSA26 Cre reporter strain. Nat Genet 1999;21:70–71. [PubMed: 9916792]

Soufan AT, van den Hoff MJ, Ruijter JM, de Boer PA, Hagoort J, Webb S, Anderson RH, Moorman AF. Reconstruction of the patterns of gene expression in the developing mouse heart reveals an architectural arrangement that facilitates the understanding of atrial malformations and arrhythmias. Circ Res 2004;95:1207–1215. [PubMed: 15550689]

Verzi MP, McCulley DJ, De Val S, Dodou E, Black BL. The right ventricle, outflow tract, and ventricular septum comprise a restricted expression domain within the secondary/anterior heart field. Dev Biol 2005;287:134–145. [PubMed: 16188249]

Waldo KL, Kumiski DH, Wallis KT, Stadt HA, Hutson MR, Platt DH, Kirby ML. Conotruncal myocardium arises from a secondary heart field. Development 2001;128:3179–3188. [PubMed: 11688566]

Washington Smoak I, Byrd NA, Abu-Issa R, Goddeeris MM, Anderson R, Morris J, Yamamura K, Klingensmith J, Meyers EN. Sonic hedgehog is required for cardiac outflow tract and neural crest cell development. Dev Biol 2005;283:357–372. [PubMed: 15936751]

Webb S, Brown NA, Anderson RH. Formation of the atrioventricular septal structures in the normal mouse. Circ Res 1998;82:645–656. [PubMed: 9546373]

Webb S, Anderson RH, Lamers WH, Brown NA. Mechanisms of deficient cardiac septation in the mouse with trisomy 16. Circ Res 1999;84:897–905. [PubMed: 10222336]

Wessels A, Anderson RH, Markwald RR, Webb S, Brown NA, Viragh S, Moorman AF, Lamers WH. Atrial development in the human heart: an immunohistochemical study with emphasis on the role of mesenchymal tissues. Anat Rec 2000;259:288–300. [PubMed: 10861362]

Zhang XM, Ramalho-Santos M, McMahon AP. Smoothened mutants reveal redundant roles for Shh and Ihh signaling including regulation of L/R symmetry by the mouse node. Cell 2001;106:781–792. [PubMed: 11517919]

Zucker RM, Hunter ES 3rd, Rogers JM. Apoptosis and morphology in mouse embryos by confocal laser scanning microscopy. Methods 1999;18:473–480. [PubMed: 10491277]

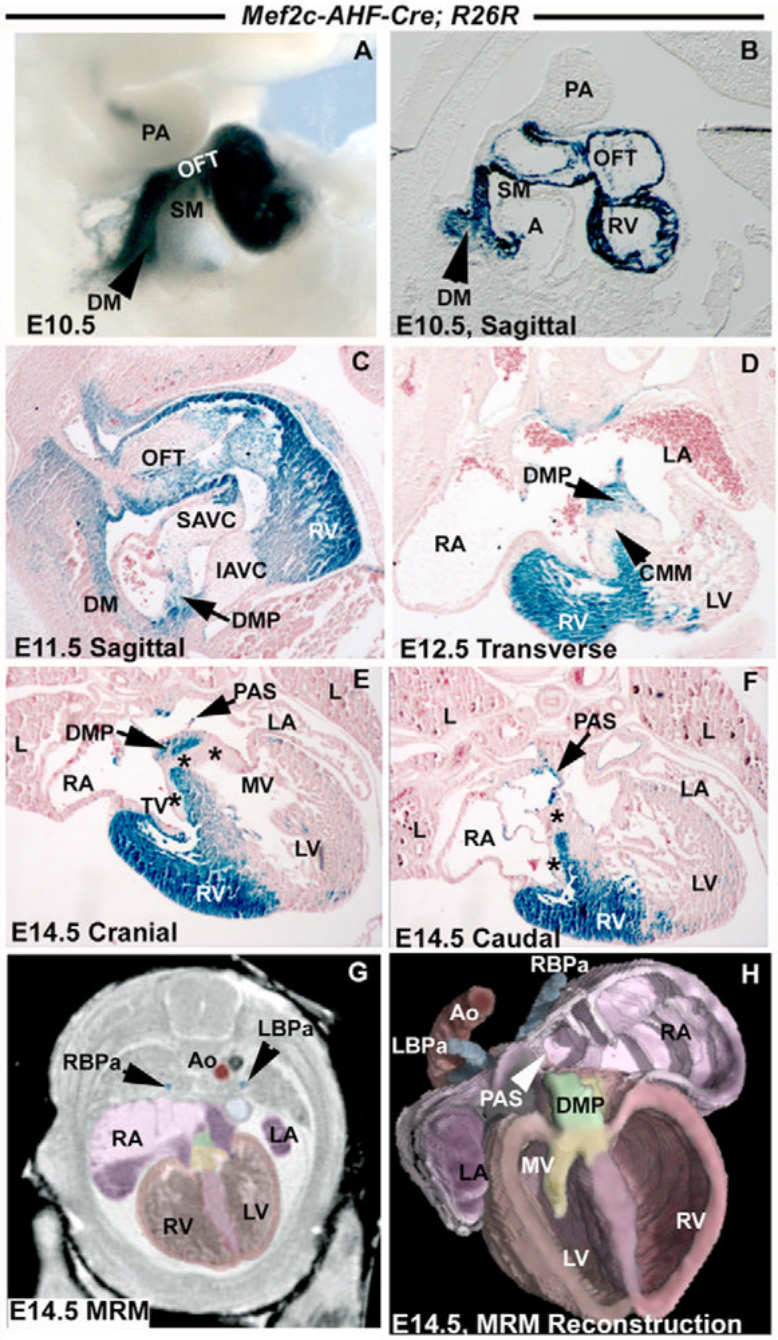

Fig. 1. DM contributions to atrial septation are marked by *Mef2C-AHF-Cre*

(**A–F**) *Mef2C-AHF-Cre* mediated *R26R* expression. Whole-mount (A) and sagittal section (B) at E10.5 demonstrates DM expression leading into the atria. (C) At E11.5 DM expression is continuous with the DMP in the atria. (D) Transverse E12.5 section demonstrates interface between the DMP and AV cushion-derived CMM. (E, F) Transverse sections at E14.5 show expression in DMP and PAS but not in AV cushion derived tissues. (**G**, **H**) Comparison of *Mef2C-AHF-Cre; R26R* transverse sections and MRM slices enabled 3D MRM reconstruction of the heart. (G) Sample color-labeled transverse slice demonstrating labeling scheme used for renderings. (H) 3D reconstruction depicts heart from a dorsal-lateral perspective with AV cushion-derived tissue labeled yellow and DMP labeled green. A, atria; Ao, aorta; CMM,

central mesenchymal mass; DM, dorsal mesocardium; DMP, dorsal mesenchymal protrusion; IAVC, inferior atrioventricular cushion; L, lung; LA, left atria; LBPa, left branch pulmonary artery; LV, left ventricle; MV, mitral valve; OFT, outflow tract; PA pharyngeal arch; PAS, primary atrial septum; RA, right atria; RBPa, right branch pulmonary artery; RV, right ventricle; SAVC, superior atrioventricular cushion; SM, splanchnic mesoderm; TV, tricuspid valve.

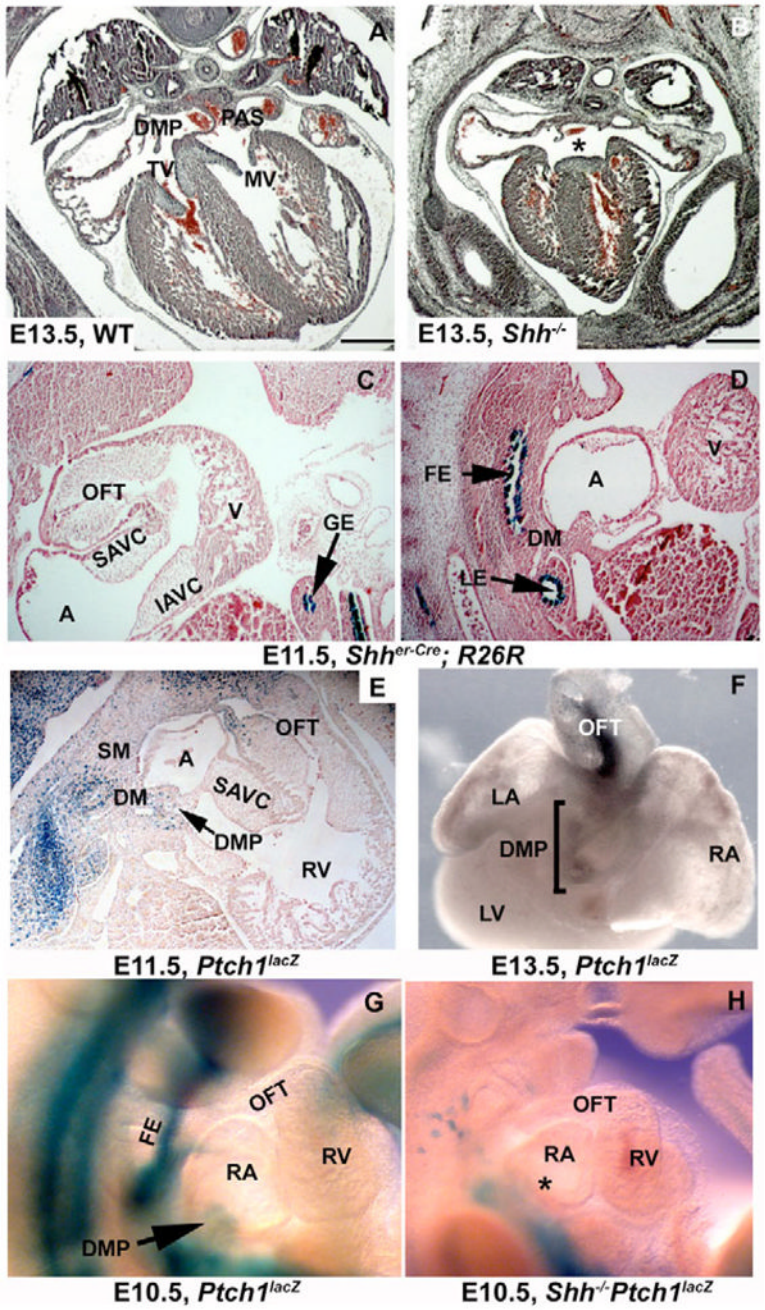

Fig. 2. *Shh*$^{-/-}$ mutant AVSD and defective DMP development

Transverse sections of E13.5 WT (**A**) and *Shh*$^{-/-}$ mutant (**B**) demonstrate a typical AVSD (asterisk) characterized by a large atrial septal defect and abnormal AV valve openings (scale bar, 500 μm). (**C**, **D**) Sagittal sections of *Shh*$^{er-Cre}$*; R26R* e show lack of heart expression, but foregut expression (FE) is juxtaposed to the DM. (**E**) *Ptch1*^{lacZ} is observed in the DM, splanchnic mesoderm and DMP at E11.5 (sagittal section). (**F**) OFT and atrial DMP expression are the only areas of the heart where Hh activity is detected at E11.5 (wholemount, dorsal view). (**G**) E10.5 WT *Ptch1*^{lacZ} embryo shows expression in the DMP (wholemount, right view,). (**H**) E10.5 *Shh*$^{-/-}$ mutants largely lack *Ptch1*^{lacZ} expression in atria (asterisk). A, atria; FE, foregut endoderm; GE, gut endoderm; IAVC, inferior atrioventricular cushion; LE, lung

endoderm; LA, left atrium; LV, left ventricle; MV, mitral valve; PAS, primary atrial septum; RA, right atrium; RV, right ventricle; SAVC, superior atrioventricular cushion; SM, splanchnic mesoderm; TV, tricuspid valve; V, ventricle.

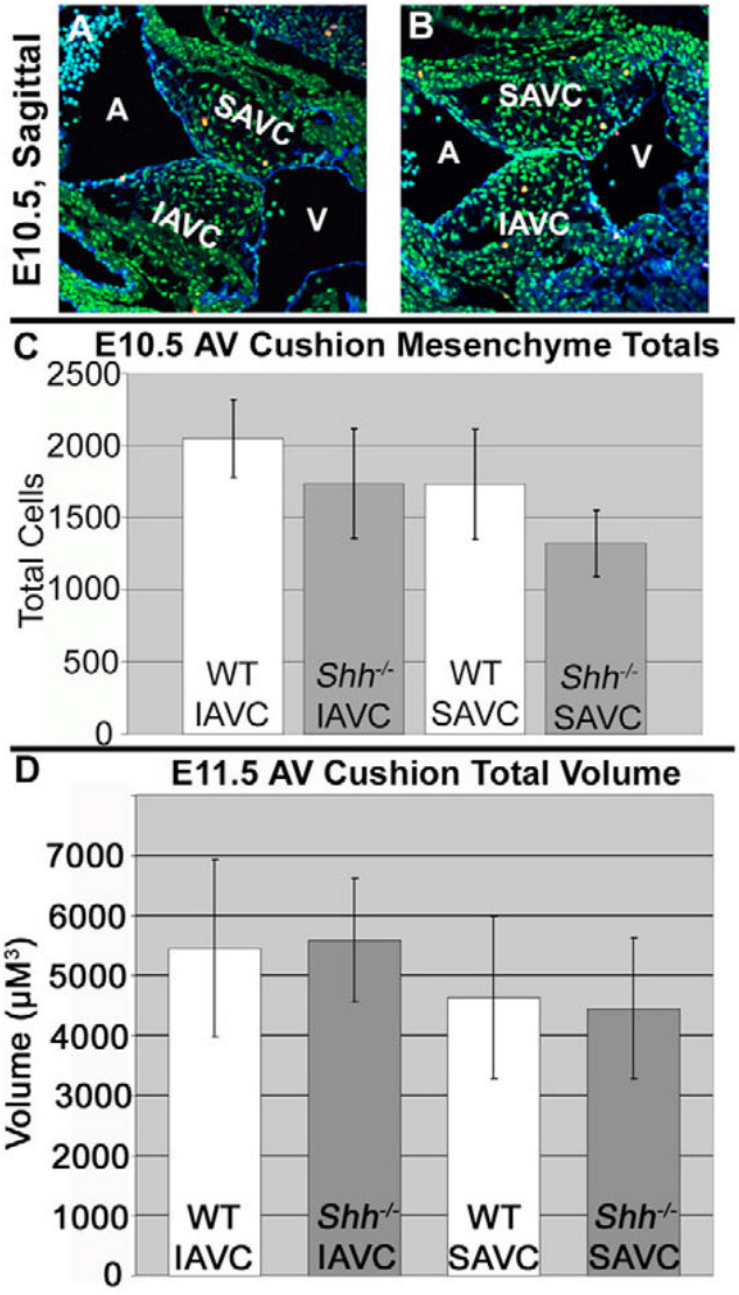

Fig. 3. AV cushion formation is normal in *Shh*$^{-/-}$ mutant embryos

Wild-type (**A**) and *Shh*$^{-/-}$ (**B**) E10.5 AV cushion sagittal sections stained with PECAM1 (blue) and nuclear marker (green) demonstrated no significant change in morphology or total mesenchyme per cushion (quantitated in **C**; wild type and *Shh*$^{-/-}$ *n*=4). Identical analysis at E11.5 found no significant change in total mesenchyme cells or cushion volume (**D**; wild type and *Shh*$^{-/-}$ *n*=3). A, atria; V, ventricle; IAVC, inferior atrioventricular cushion; SAVC, superior atrioventricular cushion.

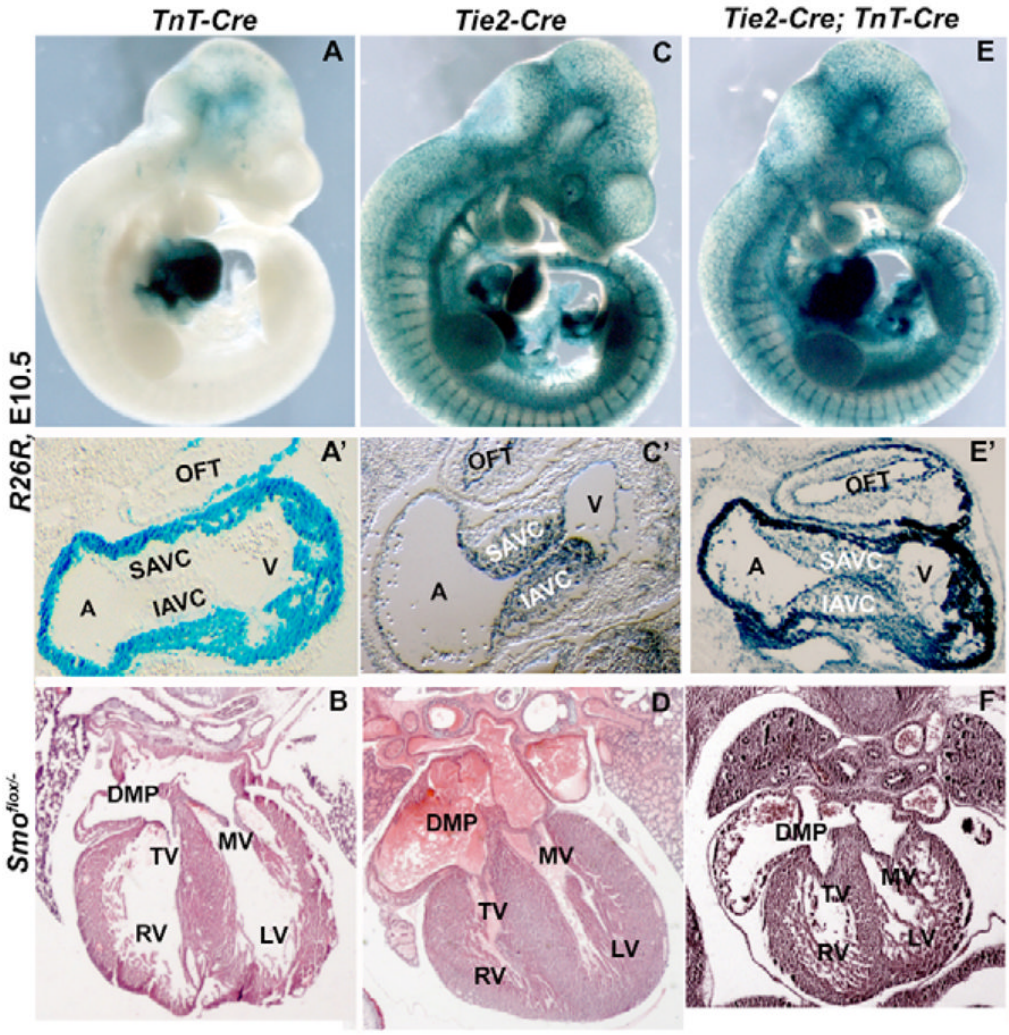

Fig. 4. The AV cushions do not require Hh signaling for normal AV septation

(**A**) *TnT-Cre* is expressed in the myocardium as detected by *R26R* β-galactosidase activity in whole-mount (A) or in sagittal section (A′) at E10.5. (**B**) Ablation of *Smo* with *TnT-Cre* results in normal AV septation (E18.5). (**C**) *Tie2-Cre* is expressed in all endothelial cells and derivatives, including AV cushion mesenchyme (C, C′). (**D**) *Tie2-Cre; Smo*$^{flox/-}$ embryos have normal AV septation (E18.5). (**E**, **F**) Simultaneous ablation of *Smo* using both *Tie2-Cre* and *TnT-Cre* (reported in E, E′) does not induce AV septation defects (F, E14.5 transverse section). A, atria; IAVC, inferior atrioventricular cushion; LV, left ventricle; MV, mitral valve; RV, right ventricle; SAVC, superior atrioventricular cushion; TV, tricuspid valve; V, ventricle.

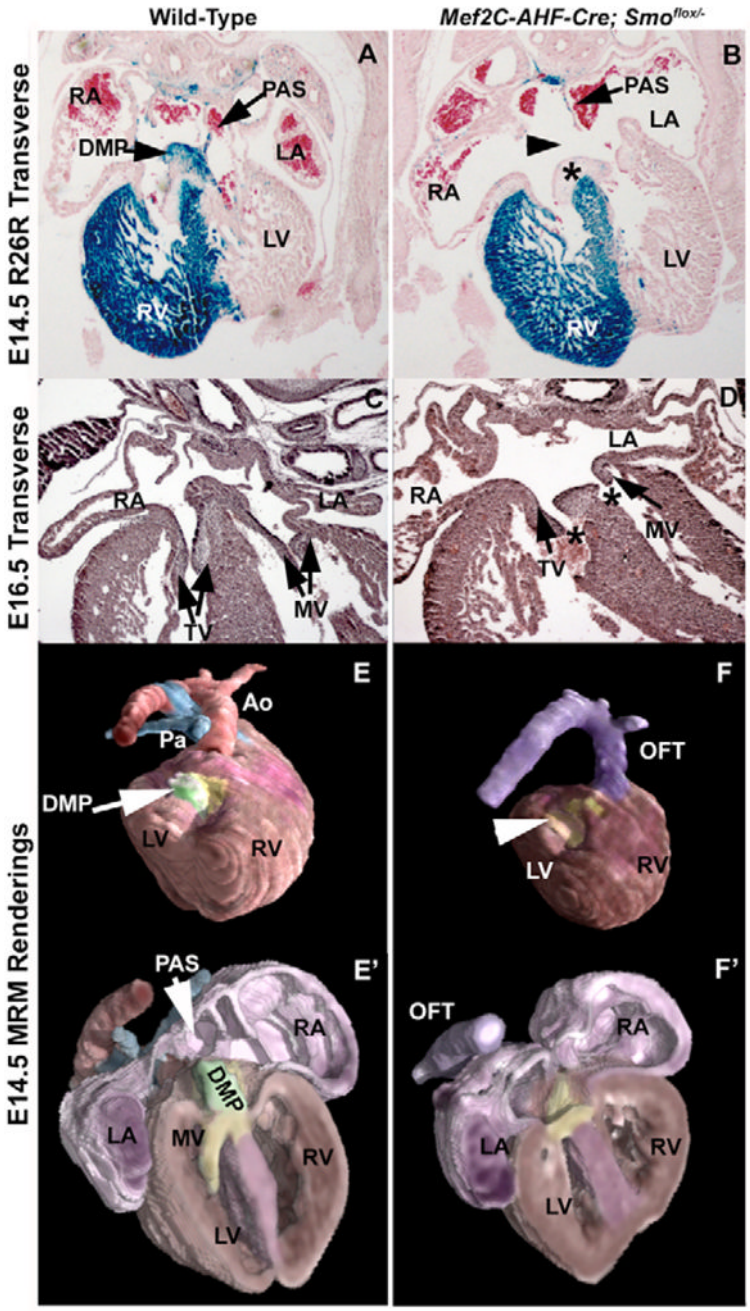

Fig. 5. Conditional ablation of *Smo* using *Mef2C-AHF-Cre* results in AVSD

E14.5 transverse sections of (**A**) WT (*Mef2C-AHF-Cre; R26R*) and (**B**) *Mef2C-AHF-Cre; R26R; Smo*$^{flox/-}$ mutant embryos. Loss of Hh receptiveness results in loss of the DMP (arrowhead in B). The central mesenchymal mass on the ventricular septum (asterisk) is more rounded with less distinct AV septal valve leaflets in mutants. (**C**, **D**) The disparity in septal valve development becomes more pronounced by E16.5. Mural leaflets (arrows in D) appear unaffected in mutants, while septal leaflets (asterisks in D) are missing. Multiple views of wild type (**E**, **E′**) and conditional mutant (**F**, **F′**) MRM renderings demonstrate loss of the DMP in addition to a single OFT vessel in mutants (purple). Atrial walls have been subtracted in E and F to allow visualization of wedge-shaped DMP (green). A section of the dorsal wall has been

subtracted in E′ and F′ to demonstrate relative size of DMP to other septal structures. Ao, aorta; LA, left atria; LV, left ventricle; MV, mitral valve; Pa, pulmonary artery; PAS, primary atrial septum; RA, right atria; RV, right ventricle; TV, tricuspid valve. Color scheme: red; aorta; brown, ventricles; yellow, AV cushion tissue; blue, pulmonary artery; purple, atria; DMP, green.

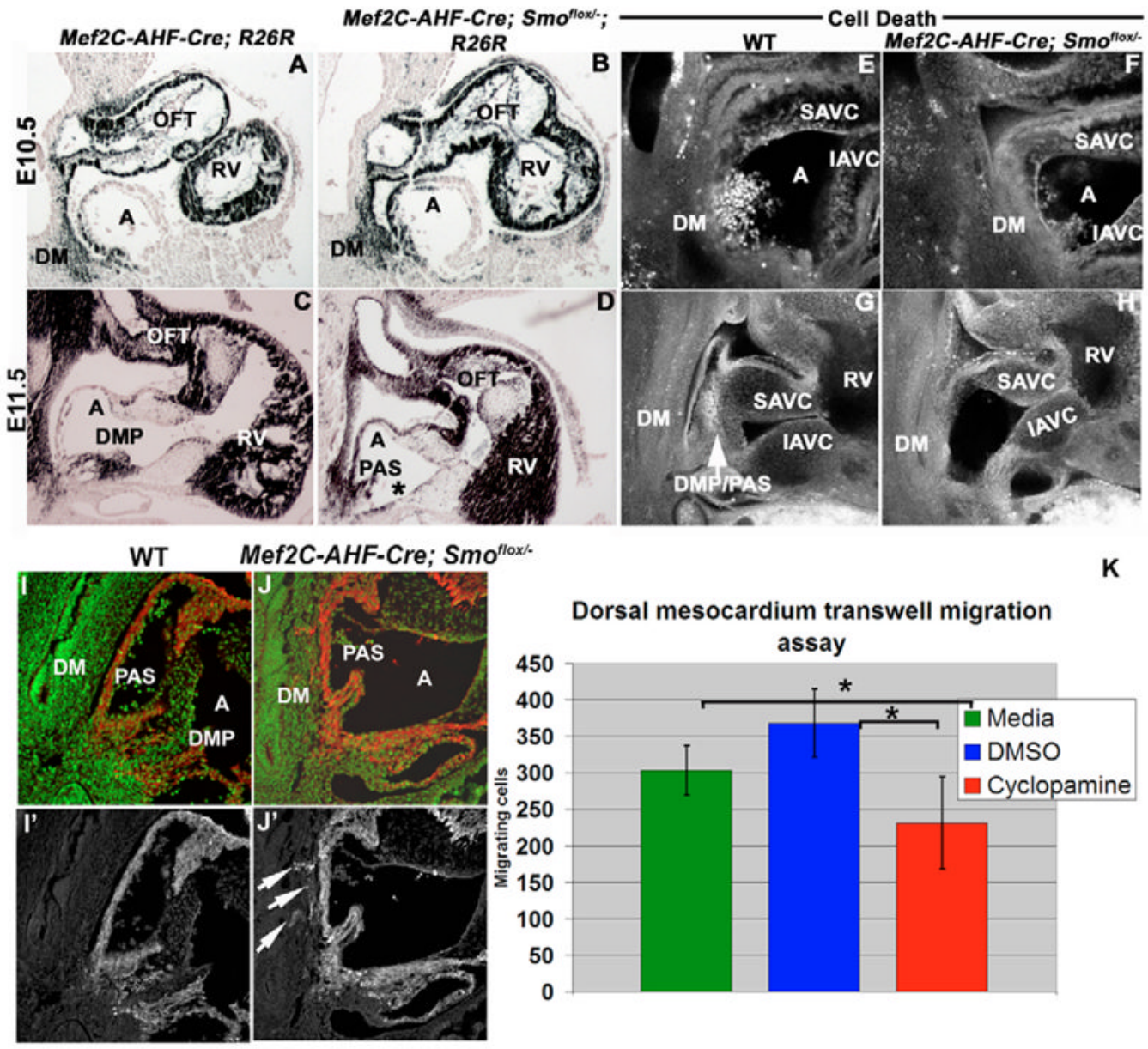

Fig. 6. Deficient Hh activity results in abnormal DM development and reduced cell motility

Mef2C-AHF-Cre; Smo$^{flox/-}$*; R26R* mutant embryos and controls are compared. β-galactosidase staining at E10.5 (**A**, **B**) demonstrates relatively normal DM levels in mutant (B). Staining at E11.5 (**C**, **D**) demonstrates loss of DMP (asterisk) while some atrial myocardial and PAS staining is maintained. (**E–H**) Lysotracker Red cell death analysis demonstrates no detectable increase in mutant embryos (F, H) when compared with controls (E, G) at E10.5 or E11.5. (**I**, **J**) Sagittal sections stained for MF-20 (red) and nuclei (green) demonstrate normal myocardial staining in the DMP and absence of MF-20 staining in DM in E11.5 wild type (I) compared with abnormal MF-20 staining within the DM of *Mef2C-AHF-Cre; Smo*$^{flox/-}$ embryos (J). MF-20 channel only (I′, J′) shows ectopic staining. (**K**) Significantly decreased DM migration is observed with 10 μM cyclopamine treatment compared with media alone or DMSO controls. A, atria; IAVC, inferior atrioventricular cushion; PAS, primary atrial septum; RV, right

ventricle; SAVC, superior atrioventricular cushion. *P=0.02 (media versus cyclopamine), *P=0.001 (DMSO versus cyclopamine).

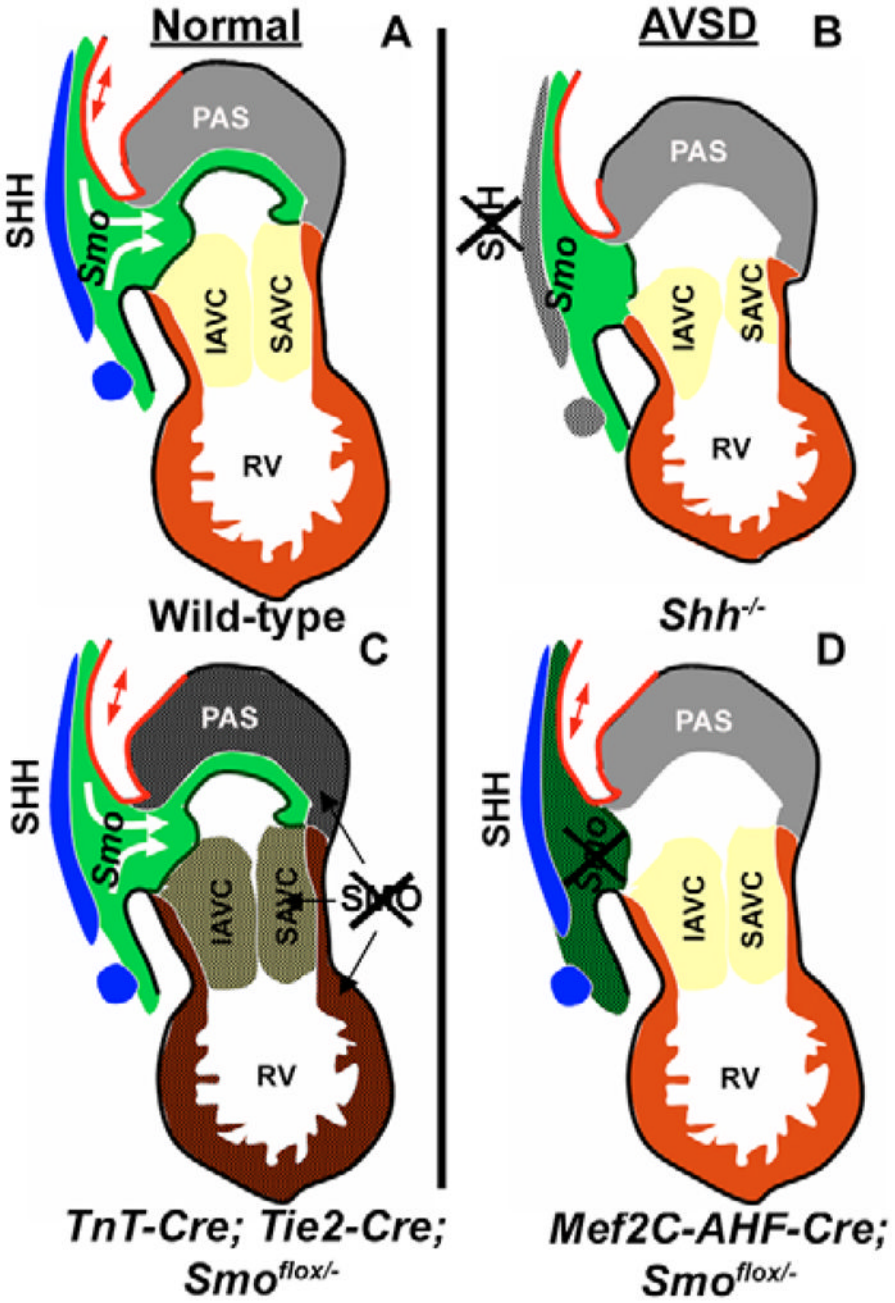

Fig. 7. Model of DMP development in mutant backgrounds

Shh has multiple roles in AV septation, depicted by schematic sagittal sections at E11.5. (**A**) Shh produced by foregut endoderm (blue) signals to adjacent DM (green) allowing for mesenchymal movement into the atria and subsequent formation of the DMP. DM-derived endocardium (dark green) and splanchnic mesoderm (red) are also added to the atria at this time. (**B**) Global loss of *Shh* results in a failure of DMP development as well as abnormal AV cushion shape, probably owing to OFT and right ventricle shortening. (**C**) Loss of receptiveness for Hh signaling in the myocardium, endocardium and mesenchyme derived from the endocardium (*TnT-Cre; Tie2-Cre; Smo*$^{flox/-}$) does not recapitulate the *Shh*-null AVSD phenotype. (**D**) While *Shh* is maintained in *Mef2C-AHF-Cre; Smo*$^{flox/-}$ mutants, lack of

receptiveness in DM leads to failure of these cells to develop into the DMP. Adapted, with permission, from Lamers and Moorman (Lamers and Moorman, 2002).